Progress In Electromagnetics Research M, Vol. 100, 175–186, 2021

Four Element Square Patch MIMO Antenna for DSRC, WLAN, and X-Band Applications

Usha D. Yalavarthi*, Ravi T. Koosam, Monica N. S. D. Venna, and Bhargav Thota

Abstract—A novel 4-element Multi-Input Multi-Output (MIMO) array antenna is proposed for Dedicated Short Range Communications (DSRC), Wireless Local Area Network (WLAN), and X-band applications. The proposed antenna is a microstrip antenna that consists of a simple square patch as radiating element with a defected ground structure (DGS). Dimensions of the proposed antenna are very compact with size $40 \times 48 \times 0.8\,\text{mm}^3$. It operates from 5.6–6.1 GHz (DSRC/WLAN) and 8.7–10.8 GHz (X-band) with impedance bandwidths ($S_{11} <= -10$ dB) of 500 MHz and 2.1 GHz, respectively. The isolation between elements of MIMO is also greater than 25 dB in the operating bands. Antenna performance parameters are investigated at 5.9 GHz and 10.5 GHz center frequencies and computer-simulated, and experimentally measured characteristics are found to be satisfactory. A peak gain of 4.8 dB is achieved, and radiation efficiency is also greater than 75% in operating bands. Envelope Correlation Coefficient (ECC) is less than 0.05, and Diversity Gain (DG) is very close to 10. Group delay among the MIMO elements is below 2.7 ns, and Channel Capacity Loss CCL is also below 0.4 bits/sec/Hz. Therefore, the proposed 4-element MIMO antenna is suggestible for DSRC/WLAN and X-band applications.

1. INTRODUCTION

The emerging applications in smart transportation systems require low cost, reliable and high performance RF systems, and low profile antennas. IEEE standard has developed DSRC band and Wireless Access in Vehicular Environment for V2X communications. Micro-strip patch antennas have low profile, easy fabrication, easy interface with RF circuitry, and can be designed for various conformable sizes and shapes. Many researchers have developed various antenna models for vehicular communications [1–13] with different substrates and structures like Liquid Crystal Polymer (LCP) based conformal and reconfigurable microstrip patch antennas. MIMO antennas are also developed for different wireless applications like vehicular and 5G in [14–18]. In this paper, a novel and compact four-element MIMO antenna is proposed with dual operating bands for DSRC, WLAN, and X-band applications. The proposed 4-element MIMO antenna contains a square patch radiator with a DGS designed using basic microstrip patch antenna design equations. Section 2 describes the single element design and its performance characteristics. MIMO antenna design, fabricated model, investigated results, and MIMO performance metrics are discussed in Section 3.

2. SINGLE ELEMENT ANTENNA

2.1. Antenna Design

A basic square patch micro-strip antenna with offset feed is designed for DSRC/WLAN and X-band applications. The proposed antenna is designed on an FR-4 substrate (dielectric constant $\varepsilon_r = 4.4$) of

Received 31 October 2020, Accepted 19 January 2021, Scheduled 23 January 2021
* Corresponding author: Usha Devi Yalavarthi (ushadevi.yalavarthi@kluniversity.in).
The authors are with the Department of ECE, Koneru Lakshmaiah Education Foundation, AP, India.

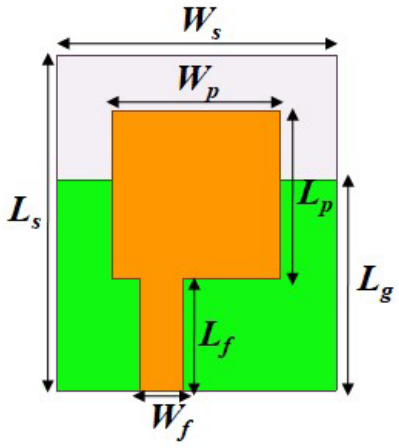

Figure 1. Geometry of proposed single element antenna.

Table 1. Design parameters of proposed single element antenna in mm.

L_s	W_s	L_p	W_p	L_g	W_f	L_f
24	20	12	12	15	3	8

thickness $t = 0.8\,\text{mm}$ and dimensions $20 \times 24\,\text{mm}^2$. Radiating patch parameters and feed width are obtained from the basic design equations of the micro-strip antenna [19, 20] as given in Equations (1) to (5). The proposed antenna geometry is illustrated in Figure 1. The final geometrical specifications of proposed single element antenna are tabulated in Table 1.

The width of micro-strip patch w_P is given by:

$$w_P = \frac{c}{2f_r}\sqrt{\frac{2}{\varepsilon_r + 1}} \tag{1}$$

where ε_r is the relative dielectric constant, and f_r is the resonant frequency.

The effective dielectric constant, $\varepsilon_{reffect}$, is calculated as:

$$\varepsilon_{reffect} = \frac{\varepsilon_r + 1}{2} + \frac{\varepsilon_r - 1}{2}\left[\left(1 + \frac{12t}{w_p}\right)^{-\frac{1}{2}} + 0.04\left(1 - \frac{w_P}{t}\right)^2\right] \tag{2}$$

The length of micro-strip patch L_p is given by:

$$L_p = \left\{\frac{c}{2f_r\sqrt{\varepsilon_{reffect}}}\right\} \tag{3}$$

Input impedance Z_{in} and width of micro-strip feed line W_f are related as:

$$Z_{in} = \frac{60}{\sqrt{\varepsilon_{reffect}}}\ln\left(\frac{8t}{W_f} + \frac{W_f}{4t}\right); \quad \text{for } \frac{W_f}{t} < 1 \tag{4}$$

$$Z_{in} = \frac{120\pi}{\sqrt{\varepsilon_{reffect}}\left[\frac{W_f}{t} + 1.393 + \frac{2}{3}\ln\left(\frac{W_f}{t} + 1.444\right)\right]}; \quad \text{for } \frac{W_f}{t} > 1 \tag{5}$$

where t is the thickness of substrate.

2.2. Results and Discussions

To optimize the performance of designed antenna, parametric analysis is performed on length of ground (DGS) L_g and feed width W_f. S_{11} characteristics of proposed single element antenna for variations in L_g and W_f are presented in Figures 2 and 3, respectively. Length of ground plane is varied from 11 mm to 19 mm with a step size of 2 mm. It is clear from Figure 2 that the proposed antenna resonates at 5.9 GHz and also at 9.1 GHz for $L_g = 15$ mm. Dual operating bands ($S_{11} <= -10$ dB) are achieved by the proposed antenna from 5.61–5.99 GHz and 8.71–10.74 GHz that are suitable for DSRC, WLAN, and X-band applications. Feed width W_f is varied from 1.0 mm to 3.0 mm with a step size of 0.5 mm. It can be observed from Figure 3 that S_{11} characteristics at 5.9 GHz and X-band are better obtained for $W_f = 3$ mm. Operating bands of the proposed antenna after parametric analysis are 5.72–6.06 GHz and 8.72–10.6 GHz.

Far filed radiation characteristics of the proposed single element antenna are investigated at 5.9 GHz and 10.5 GHz resonant frequencies. 3D gain plots and 2D radiation patterns in E-plane and H-plane are illustrated in Figures 4, 5, and 6, respectively. 3.6 dB gain is achieved at 5.9 GHz, and 4.7 dB gain is obtained at 10.5 GHz as represented in Figures 4(a) and 4(b). As observed from Figures 5(a) and 5(b),

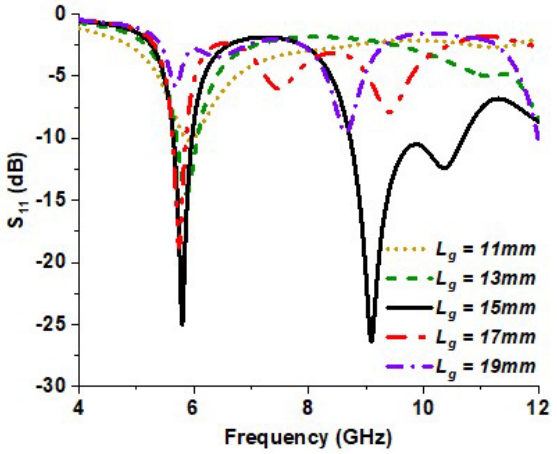

Figure 2. S_{11} characteristics of proposed single element antenna for variations in L_g.

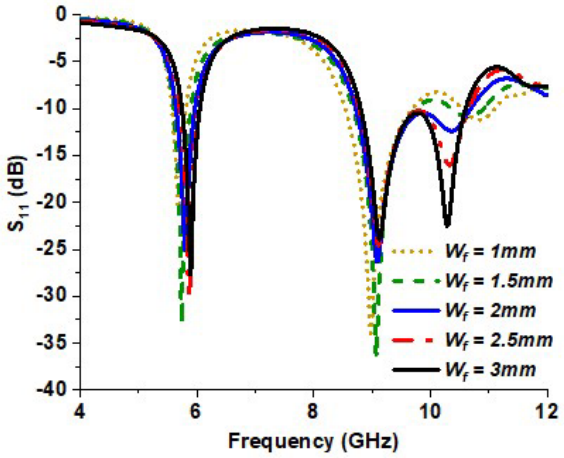

Figure 3. S_{11} characteristics of proposed single element antenna for variations in W_f.

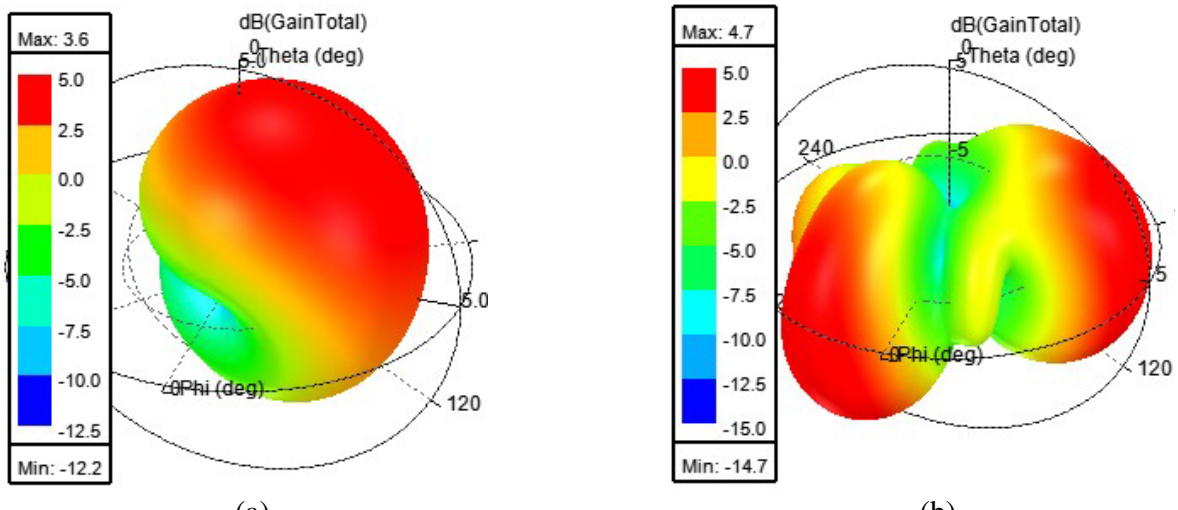

(a) (b)

Figure 4. 3D gain plots of proposed single element antenna. (a) 5.9 GHz, (b) 10.5 GHz.

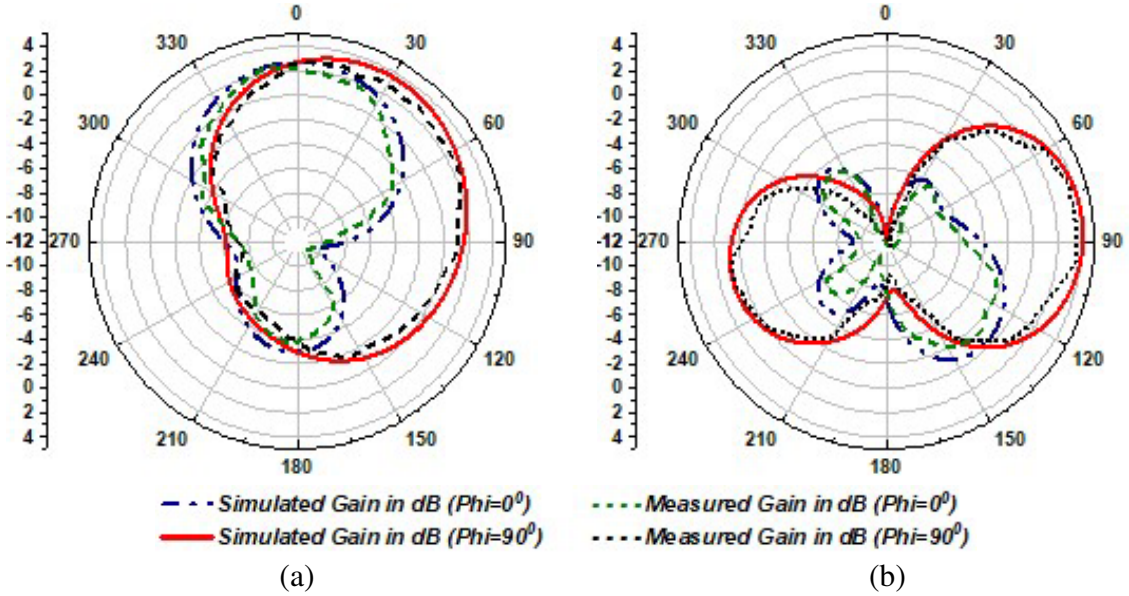

Figure 5. Radiation patterns of proposed single element antenna in E-plane. (a) 5.9 GHz, (b) 10.5 GHz.

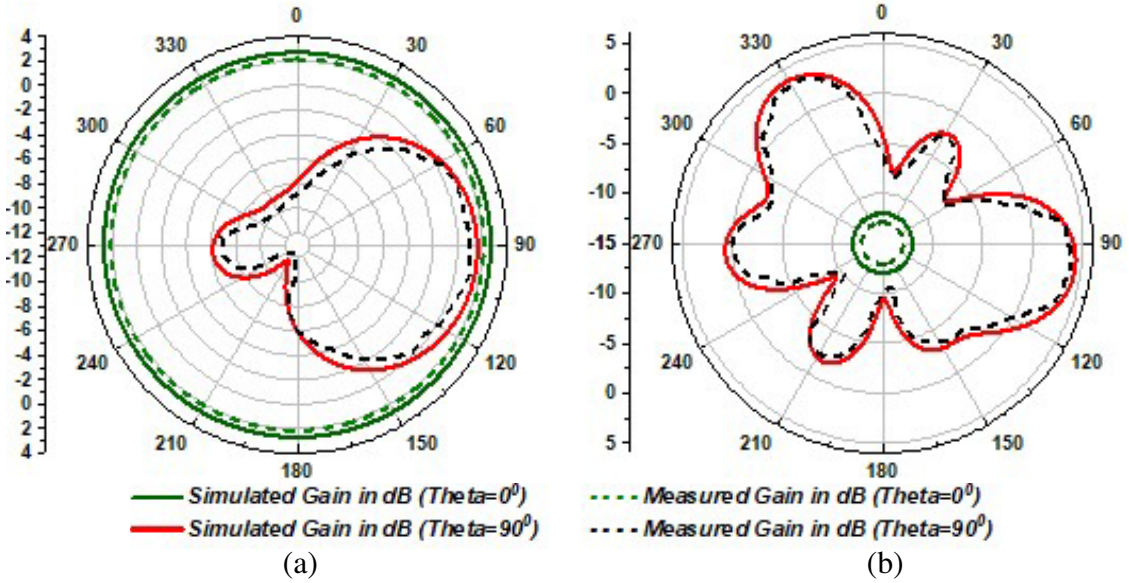

Figure 6. Radiation patterns of proposed single element antenna in H-plane. (a) 5.9 GHz, (b) 10.5 GHz.

the radiation patterns in E-plane are more directional at 10.5 GHz than 5.9 GHz frequency, and hence the gain at 10.5 GHz is enhanced. Radiation patterns in H-plane are omnidirectional at 5.9 GHz and directive in nature at 10.5 GHz.

Peak gain and radiation efficiency characteristics of the proposed single element antenna are illustrated in Figure 7. The maximum gain of 5.75 dB is obtained at 11 GHz, and the radiation efficiency of proposed antenna ranges between 70% and 80.6% in the entire operating band. By investigating antenna performance parameters at 5.9 GHz and 10.5 GHz, the proposed single element antenna is very suitable for DSRC, WLAN, and X-band applications. Simulated and experimental results are in fine agreement. To enhance spectral efficiency and channel capacity further, MIMO array antenna is designed and fabricated.

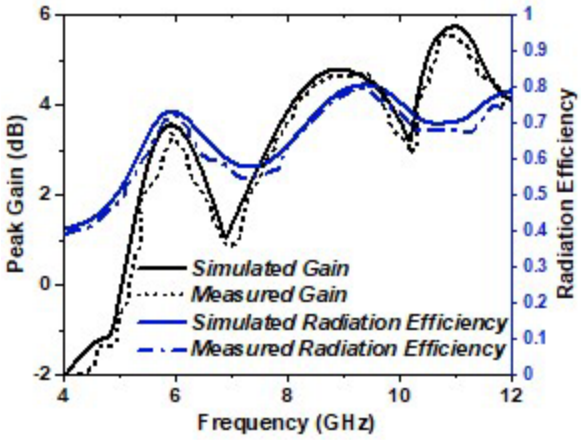

Figure 7. Gain and radiation efficiency characteristics of proposed single element antenna.

3. MIMO ARRAY ANTENNA

3.1. Two Element MIMO Antenna

A two-element collinear MIMO antenna is designed with element spacing between the elements M_1 and M_2 less than $\lambda/2$ and a gap of $W_g = 0.5\,\text{mm}$ between ground planes as presented in Figure 8(a). S-parameter characteristics of the designed 2-element collinear MIMO antenna are illustrated in Figure 8(b). As the elements M_1 and M_2 are symmetrical and identical, S_{11} and S_{22} are almost identical, and S_{12} and S_{21} are identical. From S-parameter characteristics illustrated in Figure 8(b), dual operating bands are achieved in5.75–6.05 GHz and 9.05–10.85 GHz. The mutual coupling between elements M_1 and M_2 is also less than $-30\,\text{dB}$ in the operating bands.

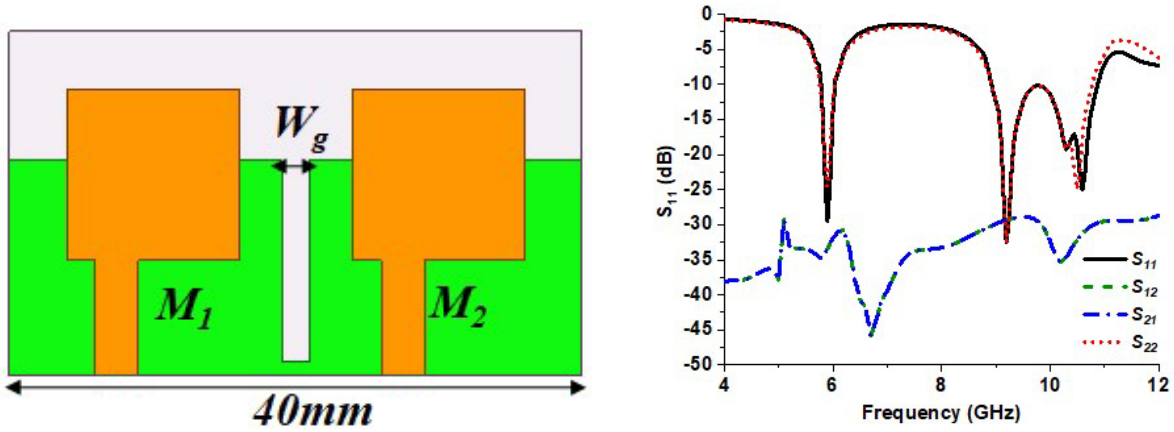

(a) (b)

Figure 8. Two-element collinear MIMO antenna. (a) Geometry, (b) S-parameter characteristics.

3.2. Four Element MIMO Antenna

A four-element MIMO antenna is designed and proposed as illustrated in Figure 9(a). The ground planes of elements M_1, M_2, M_3, and M_4 are connected through 0.5 mm strips to overcome the common reference ground plane problem among all the elements M_1, M_2, M_3, and M_4. A final dimension of the proposed antenna is $40 \times 48 \times 0.8\,\text{mm}^3$. The antenna is fabricated on an FR-4 substrate using PCB technique, and the fabricated antenna model is presented in Figure 9(b).

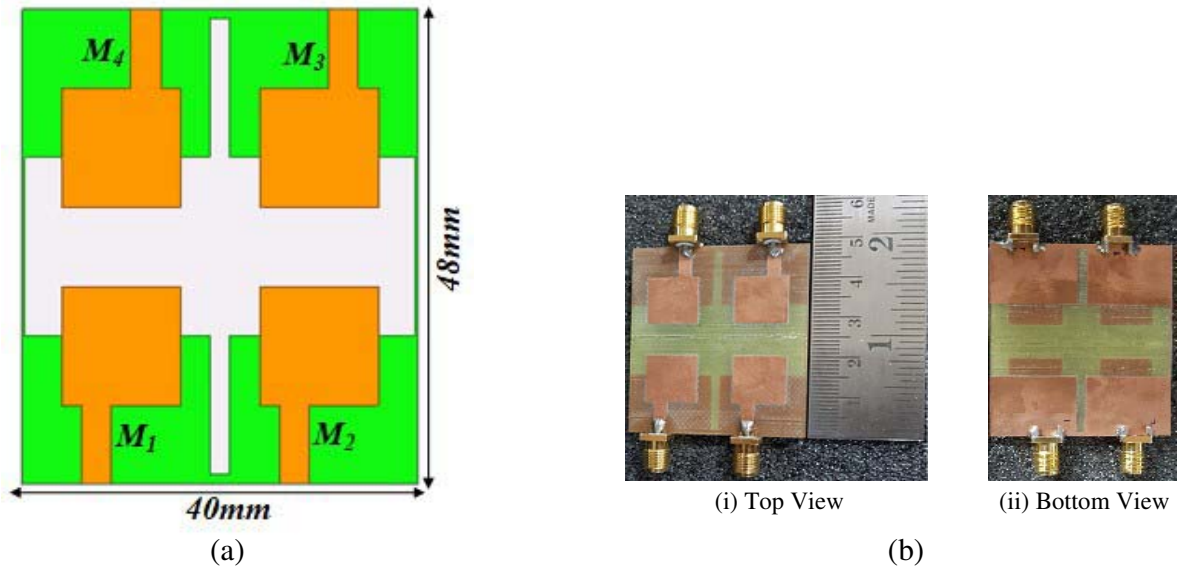

Figure 9. Proposed four-element MIMO antenna. (a) Geometry, (b) fabricated model.

3.3. Results and Discussions

Simulated and measured S-parameter characteristics of the proposed four-element MIMO array antenna with respect to Port-1 (element M_1) are illustrated in Figure 10. As the four elements are symmetrical and identical, characteristics with respect to Port-2, 3, and 4 (elements M_2, M_3, and M_4) are similar to that of Port-1 characteristics with very minute deviations. Dual operating bands are achieved by the proposed antenna. The proposed MIMO antenna operates in 5.6–6.1 GHz and 8.7–10.8 GHz with impedance bandwidths ($S_{11} <= -10$ dB) of 500 MHz and 2.1 GHz. The isolation between elements (M_1, M_2), (M_1, M_3), and (M_1, M_4) is also greater than 25 dB in operating bands. Therefore, the proposed four-element MIMO array antenna is very suitable for DSRC, WLAN, and X-band applications with minimum isolation between MIMO elements M_1, M_2, M_3, and M_4.

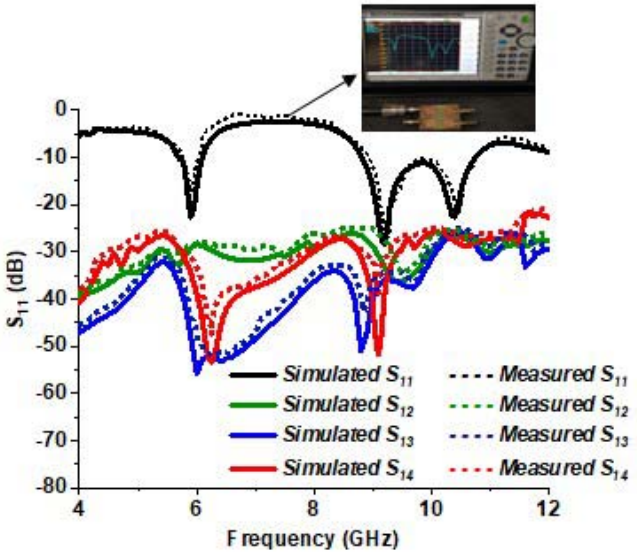

Figure 10. S-parameter characteristics of proposed 4-element MIMO antenna.

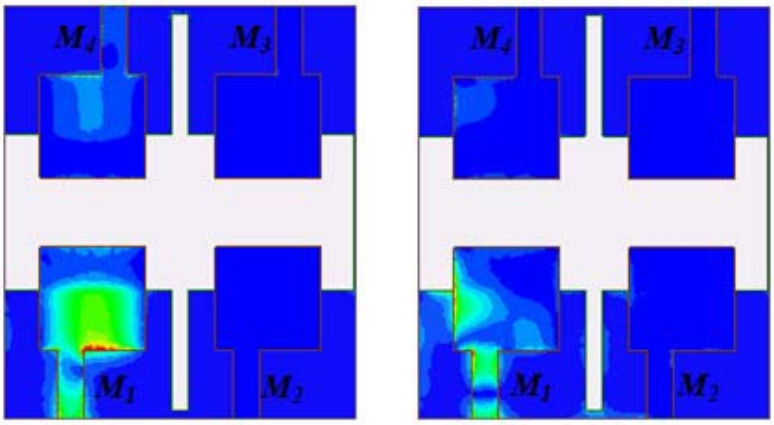

(a) (b)

Figure 11. Surface current distribution of proposed 4-element MIMO antenna for Port-1 excitation. (a) 5.9 GHz, (b) 10.5 GHz.

Surface current distributions of proposed MIMO antenna at 5.9 GHz and 10.5 GHz frequencies for Port-1 excitation are represented in Figures 11(a) and 11(b). It can be noticed that the coupling between the elements (M_1, M_2) and (M_1, M_3) is less than elements (M_1, M_4) at 5.9 GHz, and the isolations between the elements (M_1, M_3) is more than elements (M_1, M_2) and (M_1, M_4) at 10.5 GHz. The same results are also observed in S-parameter characteristics (Figure 10).

3D gain plots of the proposed MIMO antenna at 5.9 GHz and 10.5 GHz are illustrated in Figures 12(a) and 12(b). A gain of 3.64 dB is achieved at 5.9 GHz and 4.8 dB at 10.5 GHz. 2D radiation patterns of the proposed antenna in E-plane and H-plane at 5.9 GHz and 10.5 GHz resonant frequencies are presented in Figures 13 and 14, respectively. The radiation patterns at 10.5 GHz are more directional in nature with high gain than radiation patterns at 5.9 GHz.

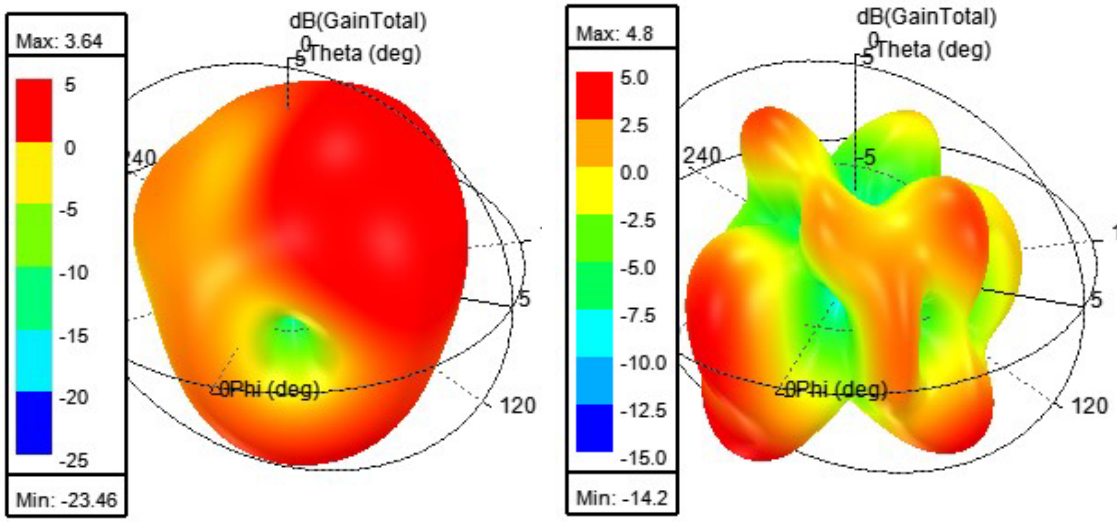

(a) (b)

Figure 12. 3D gain plots of proposed 4-element MIMO antenna. (a) 5.9 GHz, (b) 10.5 GHz.

Figure 15 represents simulated axial ratio (dB) characteristics of the proposed MIMO antenna. From these axial ratio characteristics, it is observed that the proposed MIMO antenna is linearly polarized in operating bands as axial ratio value is greater than 3 dB.

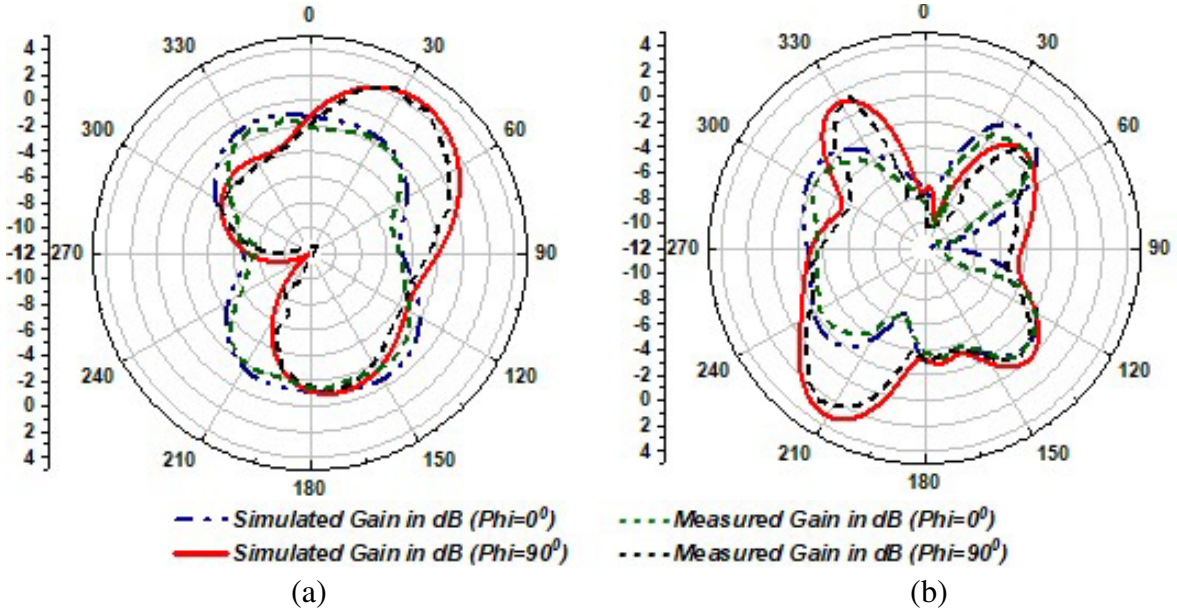

Figure 13. Radiation patterns of proposed 4-element MIMO antenna in E-plane. (a) 5.9 GHz, (b) 10.5 GHz.

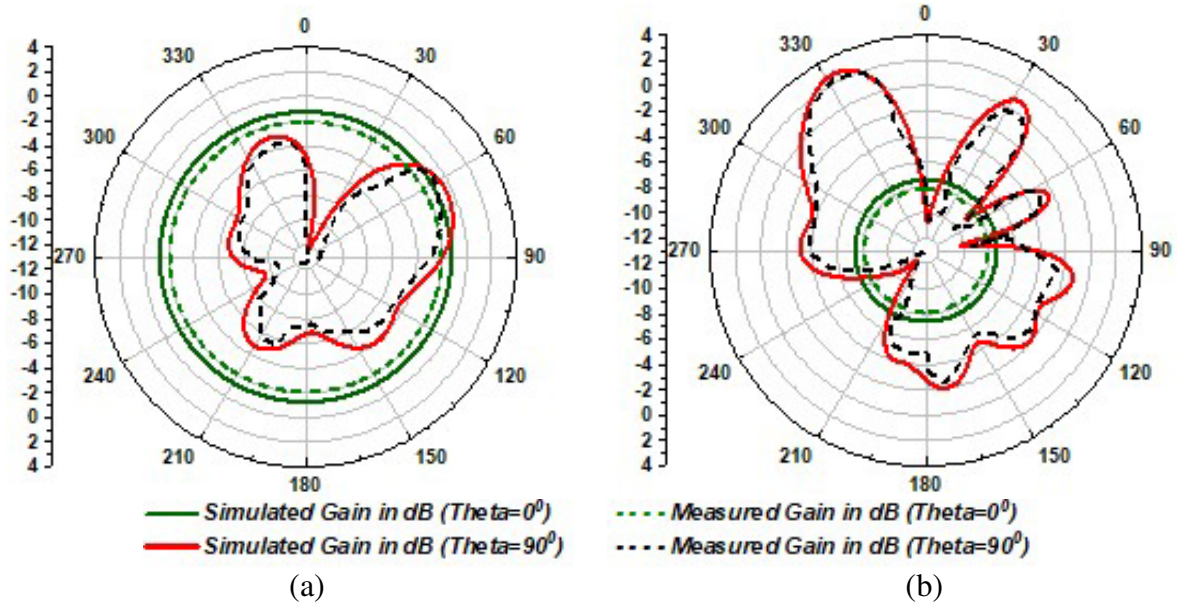

Figure 14. Radiation patterns of proposed 4-element MIMO antenna in H-plane. (a) 5.9 GHz, (b) 10.5 GHz.

Figure 16 illustrates simulated and experimental peak gain and radiation efficiency characteristics of the proposed MIMO antenna. Maximum gain of 4.8 dB is obtained at 10.5 GHz, and the radiation efficiency lies in the range of 70–79.5%. Group delay characteristics describe the time behavior of MIMO antenna. Figure 17 presents the measured group delay characteristics of proposed MIMO antenna. In the entire operating band, group delay between the elements (M_1, M_2), (M_1, M_3), and (M_1, M_4) is less than 2.7 ns. Therefore, the proposed MIMO antenna has good time domain behavior.

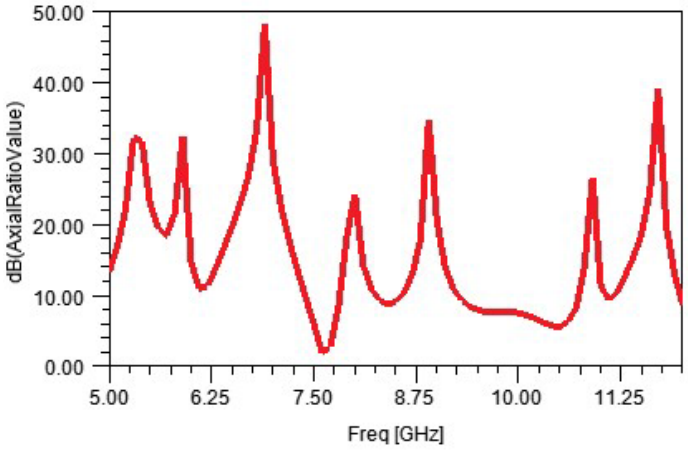

Figure 15. Simulated axial ratio characteristics of proposed MIMO antenna.

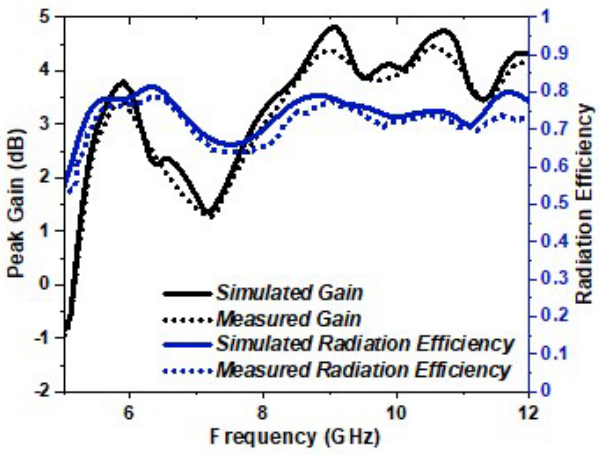

Figure 16. Gain and radiation efficiency characteristics of proposed 4-element MIMO antenna.

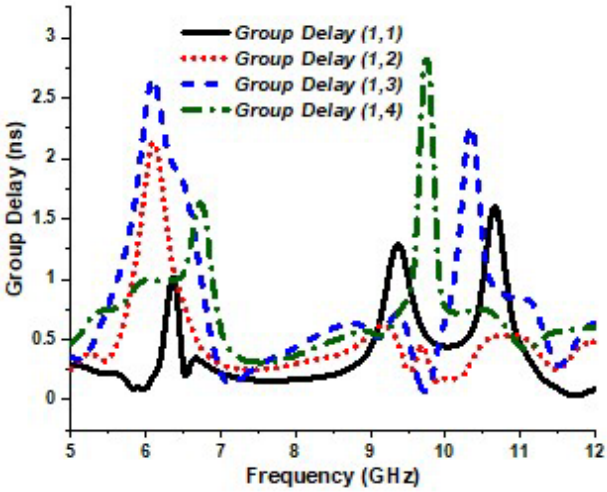

Figure 17. Group delay characteristics of proposed 4-element MIMO antenna.

3.4. MIMO Performance Parameters

Envelope Correlation Coefficient (ECC), Diversity Gain (DG), Total Active Reflection Coefficient (TARC), and Channel capacity Loss (CCL) are performance metrics of a MIMO antenna. Figure 18 illustrates the measured ECC and DG characteristics of proposed MIMO antenna. ECC between two ports can be measured from radiation patterns [17] as given in Equation (6).

$$\mathrm{ECC} = \frac{\left|\int_0^{2\pi}\int_0^{\pi}\left(\mathrm{XPR}\,E_{\theta 1}E_{\theta 2}^{*}P_{\theta}+E_{\varphi 1}E_{\varphi 2}^{*}P_{\varphi}\right)d\Omega\right|^2}{\int_0^{2\pi}\int_0^{\pi}\left(\mathrm{XPR}\,E_{\theta 1}E_{\theta 1}^{*}P_{\theta}+E_{\varphi 1}E_{\varphi 1}^{*}P_{\varphi}\right)d\Omega\times\int_0^{2\pi}\int_0^{\pi}\left(\mathrm{XPR}\,E_{\theta 2}E_{\theta 2}^{*}P_{\theta}+E_{\varphi 2}E_{\varphi 2}^{*}P_{\varphi}\right)d\Omega} \tag{6}$$

In the operating bands, ECC (1,2) and ECC (1,3) values are less than 0.05, and ECC (1,4) value is less than 0.1. The diversity gain of a MIMO antenna is defined using Equation (7). Figure 18 illustrates the simulated and measured DG characteristics of proposed MIMO antenna between the elements (M_1, M_2), (M_1, M_3), and (M_1, M_4). DG is greater than 9.99 in the operating bands.

$$\mathrm{DG} = 10\sqrt{1-\mathrm{ECC}^2} \tag{7}$$

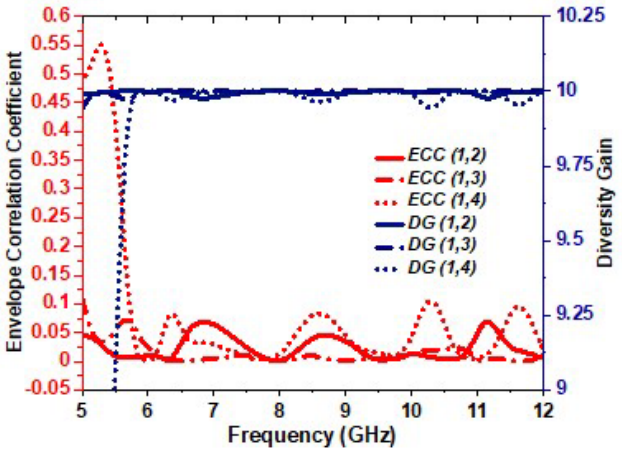

Figure 18. ECC and DG characteristics of proposed 4-element MIMO antenna.

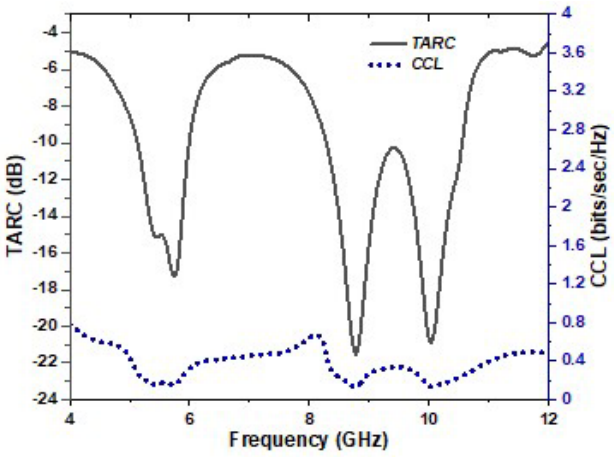

Figure 19. TARC and CCL characteristics of proposed 4-element MIMO antenna.

Figure 19 represents measured TARC characteristics and CCL of the proposed MIMO antenna. The effective operating characteristics of MIMO antenna can be described using TARC characteristics. For a two-port network, TARC can be calculated using Equation (8).

$$a^t = \sqrt{\frac{\left(\left(|S_{11} + S_{12}e^{j\theta}|^2\right) + \left(|S_{21} + S_{22}e^{j\theta}|^2\right)\right)}{2}} \tag{8}$$

where θ is the input feeding phase.

CCL parameter characterizes the channel capacity of a MIMO system. To have the fine diversity performance of the MIMO antenna, CCL value should be less than 0.4 bps/Hz. From Figure 19, it can be noticed that CCL in operating band is below 0.4 bps/Hz. Therefore, the proposed four-element MIMO antenna has good diversity performance.

3.5. Comparison

A comparison of the proposed MIMO antenna with other MIMO antennas is presented in Table 2 to describe the novelty of proposed work. The proposed four-element MIMO antenna achieves better isolation and ECC values. CCL characteristics of proposed antenna are also presented in this paper.

Table 2. Comparison of proposed antenna with other MIMO antennas.

Ref. No.	Substrate	Gain (dB)	Efficiency (%)	ECC	Isolation (dB)	CCL (bps/Hz)	Applications
M. Gulam Nabi Alsath [15]	FR4	5.0	80	< 0.09	> 24	NA	Vehicular Networks
Mohssine El Ouahabi [17]	FR4	NA	80	< 0.07	> 22	NA	Wireless
Haiyan Piao [18]	FR4	NA	NA	< 0.1	> 20	NA	5G
Proposed	FR4	4.8	> 75	< 0.05	> 25	< 0.4	DSRC, X-band

4. CONCLUSION

This paper describes a novel dual-band compact 4-element MIMO antenna for DSRC/WLAN and X-band applications. The proposed MIMO antenna is fabricated on an FR-4 substrate of dimensions $40 \times 48 \times 0.8\,\text{mm}^3$ with dielectric constant $\varepsilon_r = 4.4$. It achieves dual operating bands in 5.6–6.1 GHz (DSRC/WLAN) and 8.7–10.8 GHz (X-band) with impedance bandwidths ($S_{11} <= -10\,\text{dB}$) of 500 MHz and 2.1 GHz, respectively. The mutual coupling between MIMO elements is less than $-25\,\text{dB}$. S-parameter characteristics, surface current distribution, far filed radiation characteristics, and MIMO performance metrics of the proposed MIMO antenna are analyzed and presented in the paper. Results are investigated at 5.9 GHz (DSRC/WLAN) and 10.5 GHz (X-band) center frequencies. ECC among elements is less than 0.05, and DG is close to 10. CCL is found to be less than 0.4 bits/sec/Hz, and group delay is less than 2.7 ns. A peak gain of 4.8 dB is achieved at 10.5 GHz, and the radiation efficiency is also greater than 75%. The proposed MIMO antenna has superior isolation, low ECC, and fine diversity characteristics. Therefore, it is suggested as a suitable aspirant for DSRC/WLAN and X-band applications.

REFERENCES

1. Ijiguchi, T., D. Kanemoto, K. Yoshitomi, K. Yoshida, A. Ishikawa, S. Fukagawa, N. Kodama, A. Tahira, and H. Kanaya, "Circularly polarized one-sided directional slot antenna with reflector metal for 5.8-GHz DSRC operations," *IEEE Antennas and Wireless Propagation Letters*, Vol. 13, 778–781, 2014.
2. Mondal, T., S. Samanta, R. Ghatak, and S. R. Bhadra Chaudhuri, "A novel tri-band hexagonal microstrip patch antenna using modified Sierpinski fractal for vehicular communication," *Progress In Electromagnetics Research C*, Vol. 57, 25–34, 2015.
3. Navarro-Méndez, D. V., L. F. Carrera-Suárez, D. Sánchez-Escuderos, M. Cabedo-Fabrés, M. Baquero-Escudero, M. Gallo, and D. Zamberlan, "Wideband double monopole for mobile, WLAN and C2C services in vehicular applications," *IEEE Antennas and Wireless Propagation Letters*, Vol. 16, 16–19, 2016.
4. Naik, K. K. and P. A. V. Sri, "Design of hexadecagon circular patch antenna with DGS at Ku band for satellite communications," *Progress In Electromagnetics Research M*, Vol. 63, 163–173, 2018.
5. Madhav, B. T. P., T. Anilkumar, and S. K. Kotamraju, "Transparent and conformal wheel-shaped fractal antenna for vehicular communication applications," *AEU-International Journal of Electronics and Communications*, Vol. 91, 1–10, 2018.
6. Naik, K. K., "Asymmetric CPW-fed SRR patch antenna for WLAN/Wimax applications," *AEU-International Journal of Electronics and Communications*, Vol. 93, 103–108, 2018.
7. Prudhvi Nadh, B., B. T. P. Madhav, M. Siva Kumar, M. Venkateswara Rao, and T. Anilkumar, "Asymmetric ground structured circularly polarized antenna for ISM and WLAN band applications," *Progress In Electromagnetics Research M*, Vol. 76, 167–175, 2018.
8. Madhav, B. T. P. and T. Anilkumar, "Design and study of multiband planar Wheel-like fractal antenna for vehicular communication applications," *Microwave and Optical Technology Letters*, Vol. 60, 1985–1993, 2018.
9. Raju, M. P., D. S. Phani Kishore, and B. T. P. Madhav, "CPW FED T-shaped wearable antenna for ISM band, Wi-Fi, Wimax, WLAN and fixed satellite service applications," *Journal of Electromagnetic Engineering and Science*, Vol. 19, 140–146, 2019.
10. Joshi, M. P. and V. J. Gond, "Design and analysis of microstrip patch antenna for WLAN and vehicular communication," *Progress In Electromagnetics Research C*, Vol. 97, 163–176, 2019.
11. Bandi, S., B. T. P. Madhav, D. K. Nayak, and S. S. M. Reddy, "Compact flexible inkjet-printing antenna on paper and transparent pet substrate materials for vehicular instrument communication," *Journal of Instrumentation*, Vol. 14, 2019.
12. Dattatreya, G. and K. K. Naik, "A low volume flexible CPW-FED elliptical-ring with split-triangular patch dual-band antenna," *International Journal of RF and Microwave Computer-Aided Engineering*, Vol. 29, 2019.

13. Anilkumar, T., B. T. P. Madhav, M. Venkateswara Rao, and B. Prudhvi Nadh, "Bandwidth reconfigurable antenna on a liquid crystal polymer substrate for automotive communication applications," *AEU-International Journal of Electronics and Communications*, Vol. 117, 153096, 2020.
14. Kwon, O.-Y., R. Song, and B.-S. Kim, "A fully integrated shark-fin antenna for MIMO-LTE, GPS, WLAN, and WAVE applications," *IEEE Antennas and Wireless Propagation Letters*, Vol. 17, 600–603, 2018.
15. Alsath, M. G. N., H. Arun, Y. P. Selvam, M. Kanagasabai, S. Kingsly, S. Subbaraj, R. Sivasamy, S. K. Palaniswamy, and R. Natarajan, "An integrated tri-band/UWB polarization diversity antenna for vehicular networks," *IEEE Transactions on Vehicular Technology*, Vol. 67, 5613–5620, 2018.
16. Venkateswara Rao, M., B. T. P. Madhav, J. Krishna, Y. U. Devi, T. Anilkumar, and B. P. Nadh, "CSRR-loaded T-shaped MIMO antenna for 5G cellular networks and vehicular communications," *International Journal of RF and Microwave Computer-Aided Engineering*, Vol. 29, 2019.
17. El Ouahabi, M., A. Zakriti, M. Essaaidi, A. Dkiouak, and H. Elftouh, "A miniaturized dual-band MIMO antenna with low mutual coupling for wireless applications," *Progress In Electromagnetics Research C*, Vol. 93, 93–101, 2019.
18. Piao, H., Y. Jin, and L. Qu, "A compact and straightforward self-decoupled MIMO Antenna System for 5G applications," *IEEE Access*, Vol. 8, 129236–129245, 2020.
19. Balanis, C. A., *Antenna Theory: Analysis and Design*, 3rd edition, Wiley, New Jersey, 2005.
20. Kraus, J. D., R. J. Marhefka, and A. S. Khan, *Antennas and Wave Propagation*, 4th edition, Mc-Graw Hill, 2015.